

Cosmology in the laboratory: an analogy between hyperbolic metamaterials and the Milne universe

David Figueiredo

*Departamento de Física, Universidade Federal da Paraíba,
Caixa Postal 5008, 58051-900, João Pessoa, PB, Brazil*

Fernando Moraes*

*Departamento de Física,
Universidade Federal Rural de Pernambuco,
52171-900, Recife, PE, Brazil*

Sébastien Fumeron, Bertrand Berche

*Statistical Physics Group,
Laboratoire de Physique et Chimie Théoriques,
Université de Lorraine BP 70239,
54506 Vandœuvre les Nancy, France
(Dated: May 11, 2022)*

This article shows that the compactified Milne universe geometry, a toy model for the big crunch/big bang transition, can be realized in hyperbolic metamaterials, a new class of nanoengineered systems which have recently found its way as an experimental playground for cosmological ideas. On one side, Klein-Gordon particles, as well as probes of the Milne geometry. On the other side, the propagation of light in two versions of a liquid crystal-based metamaterial provides the analogy. It is shown that ray and wave optics in the metamaterial mimic, respectively, the classical trajectories and wave function propagation, of the Milne probes, leading to the exciting perspective of realizing experimental tests of particle tunneling through the cosmic singularity, for instance.

I. INTRODUCTION

Initial conditions are always a trouble in cosmology but can be circumvented by cyclic universe models. An endless repetition of big crunches followed by big bangs. This is in fact an old idea that can be traced back to ancient mythologies. Even without referring to initial conditions some issues remain in these models, notably the passage through the singularity, the transition from big crunch to big bang. Recently, a safe transition has been proposed [1], where the singularity is nothing more than the temporary collapse of a fifth dimension. The three space dimensions remain large and time keeps flowing smoothly. A toy model for the geometry of this transition is the compactified 2D Milne universe [2] which is essentially a double cone in 3D Minkowski spacetime. The question we want to address in this work is: can we simulate the passage through the singularity in the laboratory?

Recent advances in the field of metamaterials suggest this possibility. Arising from a pioneering idea by Veselago [3] and developed by Pendry [4], metamaterials are artificial media structured at subwavelength scales, such that their permittivity and permeability values can be tailored quasi-arbitrarily (for instance, they may exhibit negative refractive index). A particularly promising class of such media is that of hyperbolic metamaterials, for

which one of the eigenvalues of either the permittivity or the permeability tensors do not share the same sign with the two others. Hyperbolic metamaterials are now extensively studied, both for practical purpose (enhanced spontaneous emission, hyperlenses [5, 6]) but also for modeling cosmological phenomena (inflation [7], metric signature transition [8], modeling of time [9, 10]).

As far as light propagation is concerned, a $(2 + 1)$ Minkowski spacetime can be simulated with such materials. As will be seen below, the quantum dynamics of Klein-Gordon particles through the big crunch/big bang transition may be experimentally verified with light propagating in a suitable hyperbolic metamaterial.

II. THE CM UNIVERSE

In this section we will summarize the definition and features of the Milne universe and the compactified Milne universe, \mathcal{M}_C . However, firstly it is useful to analyze the geometry of a rectangular cone in \mathbb{R}^3 to get some insight. Therefore, let θ be the angle between the generatrix and the axis. In Cartesian coordinates (x, y, z) the cone surface will have the following form

$$x^2 + y^2 = z^2 \tan^2 \theta, \quad (1)$$

* Also at Departamento de Física, Universidade Federal da Paraíba, Caixa Postal 5008, 58051-900, João Pessoa, PB, Brazil

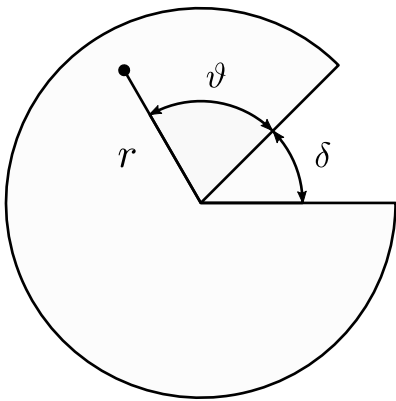


FIG. 1. Plane sector which can be bent around a cone. The deficit angle $\delta = 2\pi(1 - \sin\theta)$ reduces the range of the polar angle ϑ to $[0, 2\pi \sin\theta)$.

with parametric equations

$$x = r \sin\theta \cos(\vartheta/\sin\theta), \quad (2)$$

$$y = r \sin\theta \sin(\vartheta/\sin\theta), \quad (3)$$

$$z = r \cos\theta, \quad (4)$$

due to the fact that it is locally isometric to a piece of plane [11], where in the parametrization above $0 \leq \vartheta < 2\pi \sin\theta$ is the polar angle and $2\pi(1 - \sin\theta)$ is the deficit angle (see FIG. 1). Rescaling the polar angle as $\phi = \vartheta/\sin\theta$ one recovers the parametrization in terms of spherical coordinates (r, θ, ϕ) . Thus, the line element at the cone surface is, in terms of ϕ ,

$$ds^2 = dr^2 + r^2 \sin^2\theta d\phi^2. \quad (5)$$

Then, because $\theta = \text{constant}$ we have an induced 2D metric on the cone with the following metric tensor

$$g_{ij} = \begin{pmatrix} 1 & 0 \\ 0 & r^2 \sin^2\theta \end{pmatrix}, \quad (6)$$

where $g_{ij} = \mathbf{e}_i \cdot \mathbf{e}_j$ ($\mathbf{e}_i = \partial\mathbf{r}/\partial x^i$, $x^1 = r$, $x^2 = \phi$).

To extend the above case for the double cone, we modify the radial coordinate r making $r \rightarrow l$, so that $l \in \mathbb{R}$. Thus, $l > 0$ for the upper cone and $l < 0$ for the lower one. Making these changes in Eq. (5), we obtain the 2D induced line element for the double cone

$$ds^2 = dl^2 + l^2 \sin^2\theta d\phi^2. \quad (7)$$

Concerning the cosmological model, consider the usual Robertson-Walker line element with negative spatial curvature [12]

$$ds^2 = -dt^2 + a(t)^2 (d\chi^2 + \sinh^2\chi d\Omega^2), \quad (8)$$

where $a(t)$ is the expansion factor of the universe and $d\Omega^2 = d\theta^2 + \sin^2\theta d\phi^2$ the solid angle. For a linear expansion factor $a(t) = t$, we obtain the Milne universe metric

$$ds^2 = -dt^2 + t^2 (d\chi^2 + \sinh^2\chi d\Omega^2), \quad (9)$$

which was proposed by E.A. Milne in 1933 and represents a homogeneous, isotropic and expanding model for the universe [13] which grows faster than simple cold matter dominated or radiation dominated universes. We are interested in the hypersurfaces where $d\Omega = 0$. Then, Eq. (9) reduces to

$$ds^2 = -dt^2 + t^2 d\chi^2. \quad (10)$$

Next, we make a coordinate transformation to new variables (T, X) given by

$$T = t \cosh\chi, \quad (11)$$

$$X = t \sinh\chi, \quad (12)$$

which leads to the following form for the line element in Eq. (10), namely

$$ds^2 = -dT^2 + dX^2, \quad (13)$$

which is the usual Minkowskian metric in two dimensions. However, one must stress that the Milne universe only covers half of the Minkowski spacetime. To see why, consider the lines of constant values $\chi = \chi_0$ in Eqs. (11) and (12),

$$X = T \tanh\chi_0. \quad (14)$$

As a result, we have straight lines in a Minkowskian diagram. Taking the limits $\chi_0 \rightarrow \pm\infty$ in the equation above, one gets the light rays $X = \pm T$, which form the boundaries of the past and future light cones from the origin $(0, 0)$. Thus, one is confined in this region where $X^2 - T^2 < 0$, since the slope of the line given by Eq. (14) goes from 0 (for $\chi_0 = 0$) to ± 1 (for $\chi_0 \rightarrow \pm\infty$).

Another important point to stress is that the three dimensional space for the comoving Milne observers has infinite extension. The reason is due to the fact that the lines of constant $t = t_0$ are hyperbolas, namely

$$T^2 - X^2 = t_0^2, \quad (15)$$

and each one of the hyperbolas has infinite length. This fact is expected since the Milne universe has a negative spatial curvature [13].

Therefore, in order to compactify the Milne universe, we follow the usual approach [1, 2, 14, 15] and let the variable χ acquire some period Π . The meaning of this is as follows, in the Minkowski diagram (T, X) the lines $X = 0$ and $X = T \tanh\Pi$ should be identified as one, for instance. Therefore, because one is constrained between these two lines, the Milne universe now has a finite length and is called compactified Milne universe, \mathcal{M}_C (see FIG. 2).

Following references [16, 17], one can visualize the \mathcal{M}_C universe through a mapping into a three-dimensional Minkowski space with $ds^2 = -dz^2 + dx^2 + dy^2$, with

$$x = t\kappa \cos(\chi/\kappa), \quad (16)$$

$$y = t\kappa \sin(\chi/\kappa), \quad (17)$$

$$z = t\sqrt{1 + \kappa^2}, \quad (18)$$

where $t \in \mathbb{R}^1$ and $0 < \kappa \in \mathbb{R}^1$ is a constant parameter for compactifications (in Refs. [16, 18] it is shown that κ is related to the rapidity $\tanh^{-1} v = 2\pi\kappa$ of a finite Lorentz boost). Thus, without loss of generality, we take the period of χ as $2\pi\kappa$. Moreover, as in the previous case of the ordinary cone, we rescale χ by $\phi = \chi/\kappa$ (and hence giving a period of 2π for ϕ). Solving Eqs. (16), (17), (18) one gets the following constraint equation

$$x^2 + y^2 = \left(\frac{\kappa^2}{1 + \kappa^2} \right) z^2. \quad (19)$$

This equation is similar to Eq. (1) because the space is Euclidean for the planes $z = \text{constant}$ and also due to the periodicity of ϕ . As x, y, z can assume both positive and negative values, Eq. (19) represents a double cone with a vertex at $(0, 0, 0)$ in the 3D Minkowski space (see FIG. 3). However, due to the timelike aspect of z , the cone angle θ is a hyperbolic angle with $\tanh^2 \theta = \kappa^2/1 + \kappa^2$.

Taking into account all previous parametrizations, the parametric equations (16), (17), (18) become

$$x = t \sinh \theta \cos \phi, \quad (20)$$

$$y = t \sinh \theta \sin \phi, \quad (21)$$

$$z = t \cosh \theta, \quad (22)$$

where $\sinh \theta = \kappa$, $\cosh \theta = \sqrt{1 + \kappa^2}$ and $\phi \in \mathbb{S}^1$. As for the metric in \mathcal{M}_C ,

$$ds^2 = -dt^2 + \kappa^2 t^2 d\phi^2. \quad (23)$$

Due to the fact that the ordinary cone surface is embedded in three-dimensional Euclidean space and the \mathcal{M}_C universe has a cone surface embedded in three-dimensional Minkowski space, they share some similarities. For instance, the Milne metric tensor

$$g_{ij} = \begin{pmatrix} -1 & 0 \\ 0 & \kappa^2 t^2 \end{pmatrix}. \quad (24)$$

is similar to the two-dimensional induced metric tensor given by Eq. (6). Also, as a last comparison, let us consider the Laplace-Beltrami operator, which will be used later in this paper. Thus,

$$\Delta = \nabla_i \nabla^i = \frac{1}{\sqrt{|g|}} \partial_i \left(\sqrt{|g|} g^{ij} \partial_j \right). \quad (25)$$

where g^{ij} is the inverse metric tensor and $g = \det(g_{ij})$. From Eqs. (7) and (23), we will have

$$\Delta_{\text{Cone}} = \frac{1}{l} \frac{\partial}{\partial l} \left(l \frac{\partial}{\partial l} \right) + \frac{1}{l^2 \sin^2 \theta} \frac{\partial^2}{\partial \phi^2}, \quad (26)$$

$$\Delta_{\mathcal{M}_C} = -\frac{1}{t} \frac{\partial}{\partial t} \left(t \frac{\partial}{\partial t} \right) + \frac{1}{\kappa^2 t^2} \frac{\partial^2}{\partial \phi^2}, \quad (27)$$

which also look similar due to the resemblances between the two metrics, aside from the timelike behavior in t and the hyperbolic cone angle factor $\kappa^2 = \sinh^2 \theta$.

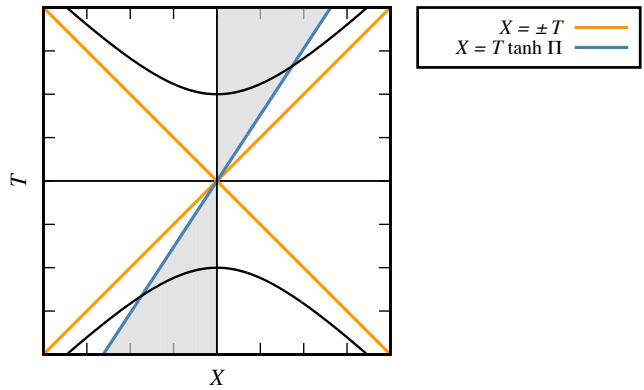


FIG. 2. Minkowski diagram showing the \mathcal{M}_C universe (gray region) delimited by the identification between the T -axis and the blue line $X = T \tanh \Pi$. The orange lines are showing the light rays $X = \pm T$ while the hyperbolas are surfaces for constant t in Eq.(15).

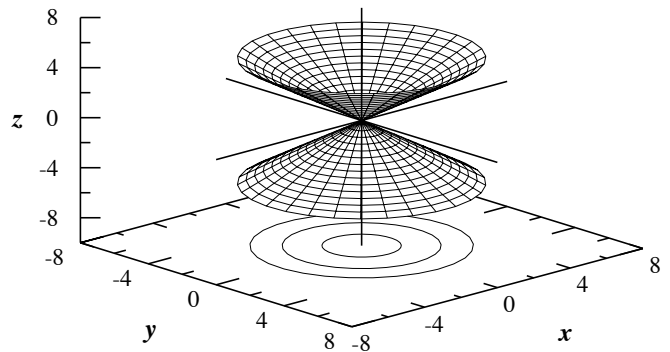


FIG. 3. Double cone surface corresponding to Eqs. (1) and (19) for 3D Euclidean space and 3D Minkowski space, respectively. The upper half part corresponds to $l, t > 0$ while the lower one is for values of $l, t < 0$.

III. CLASSICAL PARTICLE IN \mathcal{M}_C

In this section we will obtain the path followed by free classical particles (timelike geodesics) in \mathcal{M}_C . Thus, we start with the relativistic action (in natural units $c = 1$) given by [19]

$$S = -m \int \sqrt{-g_{ij} \dot{x}^i \dot{x}^j} d\lambda, \quad (28)$$

where the dot notation stands for a derivative with respect to an affine parameter λ along the curve (which can be the proper time) and $\mathcal{L}(x^i, \dot{x}^i, \lambda) = -m \sqrt{-g_{ij} \dot{x}^i \dot{x}^j}$ is the Lagrangian. The variation of the action, δS , will be

$$\delta S = -m \delta \int \sqrt{-g_{ij} \dot{x}^i \dot{x}^j} d\lambda, \quad (29)$$

thus, the least action principle $\delta S = 0$ demands that

$$\delta \int \sqrt{-g_{ij}\dot{x}^i\dot{x}^j} d\lambda = 0, \quad (30)$$

from which the geodesic equations follow

$$\ddot{x}^i + \Gamma_{jk}^i \dot{x}^j \dot{x}^k = 0, \quad (31)$$

where Γ_{jk}^i are the Christoffel symbols, namely

$$\Gamma_{jk}^i = \frac{1}{2} g^{il} (\partial_j g_{kl} + \partial_k g_{jl} - \partial_l g_{jk}). \quad (32)$$

Therefore, knowing the metric tensor g_{ij} one can calculate the Christoffel symbols to obtain the explicit form of the geodesic equations. An alternative, and more direct route to get the Christoffel coefficients, is through the Euler-Lagrange equations for the kinetic Lagrangian

$$\mathcal{L}_{\text{kin}} = \frac{1}{2} g_{ij} \dot{x}^i \dot{x}^j, \quad (33)$$

together with the Euler-Lagrange equations for \mathcal{L}_{kin} ,

$$\frac{d}{d\lambda} \left(\frac{\partial \mathcal{L}_{\text{kin}}}{\partial \dot{x}^i} \right) - \frac{\partial \mathcal{L}_{\text{kin}}}{\partial x^i} = 0, \quad (34)$$

which give the explicit geodesic equations [12] and consequently the Christoffel symbols. Thus, for the Milne metric (23), the Lagrangian will be

$$\mathcal{L}_{\text{kin}} = -\frac{\dot{t}^2}{2} + \frac{\kappa^2 t^2 \dot{\phi}^2}{2}, \quad (35)$$

and the Euler-Lagrange equations

$$\ddot{\phi} + \frac{2}{t} \dot{t} \dot{\phi} = 0, \quad (36)$$

$$\ddot{t} + \kappa^2 t \dot{\phi}^2 = 0. \quad (37)$$

From the equations above, one can see that the non-vanishing Christoffel symbols are $\Gamma_{t\phi}^{\phi} = \Gamma_{\phi t}^{\phi} = 1/t$ and $\Gamma_{\phi\phi}^t = \kappa^2 t$. Furthermore, since ϕ is a cyclic coordinate in the Lagrangian, $\partial \mathcal{L}_{\text{kin}} / \partial \phi = 0$ and the angular momentum $p_{\phi} = \partial \mathcal{L}_{\text{kin}} / \partial \dot{\phi} = \kappa^2 t^2 \dot{\phi}$ is conserved. This fact is expressed in Eq. (36).

Substituting $p_{\phi} = \kappa^2 J = \text{constant}$ in Eq. (37) and after some manipulations, the second geodesic equation becomes

$$\dot{t}^2 - \frac{\kappa^2 J^2}{t^2} = 2E, \quad (38)$$

where E is a constant of integration. The left-hand side of Eq. (38) is nothing else but minus the square modulus of the velocity $u^i = \dot{x}^i$. As a result, recalling that in special relativity one has $u^i u_i = -1$ and λ is an affine parameter, it is useful to choose $u^i u_i = -2E = -1$. Then, Eq. (38) becomes

$$\dot{t}^2 - \frac{\kappa^2 J^2}{t^2} = 1. \quad (39)$$

Solving Eq. (39) for \dot{t} , we get

$$\dot{t} = \pm \sqrt{\frac{t^2 + \kappa^2 J^2}{t^2}}, \quad (40)$$

which leads to a simple integration of the form

$$\int \frac{t dt}{\sqrt{t^2 + \kappa^2 J^2}} = \pm \int d\lambda, \quad (41)$$

and therefore to the parametric equation $t = t(\lambda)$ given by

$$t(\lambda) = \pm \sqrt{\Delta \lambda^2 - \kappa^2 J^2}, \quad (42)$$

where $\Delta \lambda = \lambda - \lambda_0$, with λ_0 being a constant of integration.

In order to obtain the parametric equation $\phi = \phi(\lambda)$, we substitute Eq. (42) in the relation $t^2 \dot{\phi} = J$ and solve for $\dot{\phi}$. Namely,

$$\dot{\phi} = \frac{J}{\Delta \lambda^2 - \kappa^2 J^2}, \quad (43)$$

leading to the following integration

$$\int d\phi = J \int \frac{d\lambda}{\Delta \lambda^2 - \kappa^2 J^2}. \quad (44)$$

As a result, the parametric equation $\phi = \phi(\lambda)$ is

$$\phi(\lambda) = \phi_0 - \frac{1}{\kappa} \coth^{-1} \left(\frac{\Delta \lambda}{\kappa J} \right), \quad (45)$$

where ϕ_0 is a constant. Combining Eqs. (42) and (45), one gets the equation of the trajectory

$$t = \pm \frac{t_0}{|\sinh \kappa \Delta \phi|}, \quad (46)$$

where $t_0 = \kappa |J|$ and $\Delta \phi = \phi - \phi_0$. The above equation is a Poincaré spiral [20], with the + (−) sign corresponding to the upper (lower) cone. Furthermore, for $J \neq 0$ one can see that depending on the choice of the signal (or sheet of the cone), the particle always remains in the upper or lower region with no link between those regions of spacetime (see FIG. 4), but for $J = 0$, which corresponds to $\phi = \phi_0$ and $t = \pm \Delta \lambda$, the geodesics are straight lines.

On the other hand, from Eqs. (11) and (12) one can see that all the trajectories given by Eq. (46) are straight lines in Minkowski spacetime,

$$X = \pm \frac{t_0}{\cosh \kappa \phi_0} + T \tanh \kappa \phi_0, \quad (47)$$

where for $J = 0$ one recovers Eq. (14). As a result, the particle indeed can travel from one cone to the other, but such trajectories are very unstable since small perturbations in the value of $J = 0$ causes large deviations on the trajectories. A similar result was found for a classical

particle in a double cone in Ref. [21], where a classical non-relativistic particle constrained to a double cone only crosses the vertex through straight lines.

However, we are dealing with a toy model for a cyclic universe with contraction and expansion phases joined by a cosmic singularity. Thus, as pointed out in Refs. [16, 17], due to the fact that timelike geodesics coincide with the trajectories of *test* particles, which do not distort the spacetime around them, there is no obstacle for such geodesics to reach (leave) the singularity. Furthermore, if one postulates that such a particle arriving at the singularity coming from the lower cone is “annihilated” at the singularity, while another one is “created” at the upper cone, and considering that the Cauchy problem is not well defined at $t = 0$, there are several types of propagation depending on the way a particle travels towards the singularity (see section 3 of Ref. [16]). Although all of them must be consistent with the constraint given by Eq. (39) and the fact that the angular momentum J is constant. It is out of the scope of this work to discuss the details and properties of such propagations.

Next we present the timelike geodesics in a polar plot, which provides a clearer way to visualize the trajectories (see FIG. 5). As already shown in FIG. 4, the trajectories in the lower cone are going towards the cosmic singularity, which means that particles in the red (orange) curve have positive (negative) angular momentum J and therefore are spinning in the counterclockwise (clockwise) direction. For the upper cone, particles traveling along the green (blue) curve have positive (negative) values of J and are spinning counterclockwise (clockwise). As a result, in a transition from the red to the green curve the angular momentum is conserved, while for a transition to the blue one, J would not be conserved. Clearly, the same reasoning applies for particles coming from the orange curve.

For the purpose of completeness, we perform the same calculations for spacelike geodesics, which can be world-lines of tachyons [22]. The procedure is the same, the major change being the choice of the constant of integration in Eq. (38). Therefore, because the momentum and velocity must be spacelike, it is useful to choose $u^i u_i = -2E = 1$. Thus, Eq. (38) becomes

$$\dot{t}^2 - \frac{\kappa^2 J^2}{t^2} = -1, \quad (48)$$

the rest of the procedure being rather straightforward and leading to the following parametric equations

$$t(\lambda) = \pm \sqrt{-\Delta\lambda^2 + \kappa^2 J^2}, \quad (49)$$

$$\phi(\lambda) = \phi_0 + \frac{1}{\kappa} \tanh^{-1} \left(\frac{\Delta\lambda}{\kappa J} \right), \quad (50)$$

where $\Delta\lambda = \lambda - \lambda_0$, with λ , λ_0 and ϕ_0 denote an affine parameter and constants of integration, respectively. As for the trajectory $t = t(\phi)$,

$$t = \pm \frac{t_0}{\cosh \kappa \Delta\phi}, \quad (51)$$

where $t_0 = \kappa |J|$ and $\Delta\phi = \phi - \phi_0$. Eq. (51) is also a Poincaré spiral, with the + (−) sign corresponding to the upper (lower) cone. Furthermore, as in the previous case the trajectories are straight lines in Minkowski spacetime,

$$X = \mp \frac{t_0}{\sinh \kappa \phi_0} + T \coth \kappa \phi_0, \quad (52)$$

where the − (+) corresponds to the upper (lower) sheet.

From Eq. (51) the variable t has t_0 as its limiting value. To clarify this result, we remark that it was pointed out by Feinberg [22] that tachyons lose energy as they speed up. Thus, from Eq. (51) the velocity $\sqrt{dx^i dx_i}/dt$ (with $i = 1, 2, 3$),

$$\left| \kappa t \frac{d\phi}{dt} \right| = \frac{t_0}{\sqrt{t_0^2 - t^2}} \quad (53)$$

ranges from $(1, \infty)$ as t ranges between 0 and t_0 , respectively (note that for a lightlike interval, $\kappa t d\phi/dt = 1$). Therefore, as the tachyon comes accelerating from the singularity, we can see from Eq. (48) that the time component of the momentum $p^0 = \dot{t}$ (which is associated with the energy) decreases, reaching its minimum value at t_0 . From that point on it starts to increase as the tachyon decelerates towards the singularity (see FIG. 6). This leads to an interpretation of tachyons being created and annihilated at the same sheet of the cone, which can be the upper sheet or the lower one. Every annihilation on a sheet creates a tachyon on the other sheet, in an endless cycle. This can be seen in a polar plot as closed curves in spacetime (see FIG. 7).

In the next section we propose a geometric optics model that emulates the trajectories of the particles in \mathcal{M}_C in a hyperbolic metamaterial.

IV. A METAMATERIAL MODEL FOR THE \mathcal{M}_C UNIVERSE

In order to simulate Milne particles in a condensed matter system, we study the propagation of light in a hyperbolic liquid crystal metamaterial, HLCCM, presented in Ref. [23]. Our study on light propagation lies in the realm of geometrical (or ray) optics, which essentially involves the application of Fermat’s principle along with the variational principle that determines the path followed by light (geodesics). Therefore we seek an extremum of the integral

$$S = \int_A^B N_e dl, \quad (54)$$

where dl is the element of arc length along the path between points A and B , N_e is the effective refractive index of the material and the product $N_e dl$ between them is called “optical path”. Because we are dealing with an anisotropic medium, there are two distinct polarizations for the light rays, namely, the ordinary and extraordinary rays. In the former, the polarization (electric field)

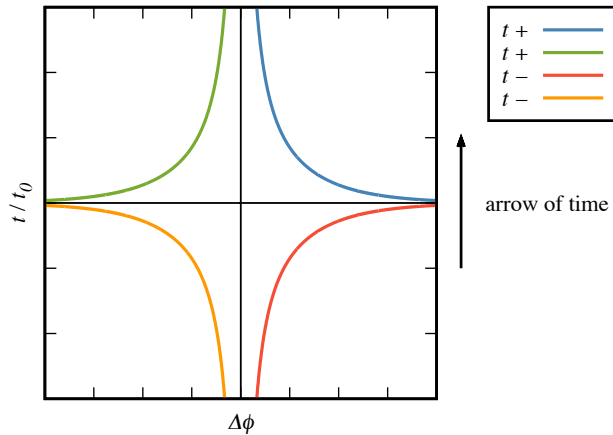


FIG. 4. Graph for the geodesic equation given by Eq. (46) with t in units of t_0 . The blue and green (orange and red) lines corresponds to trajectories in the upper (lower) cone. The arrow of time pointing up shows that time always increases, which means that in the first and third quadrants the angle ϕ decreases with time ($J < 0$), while in the second and fourth ones it increases with time ($J > 0$).

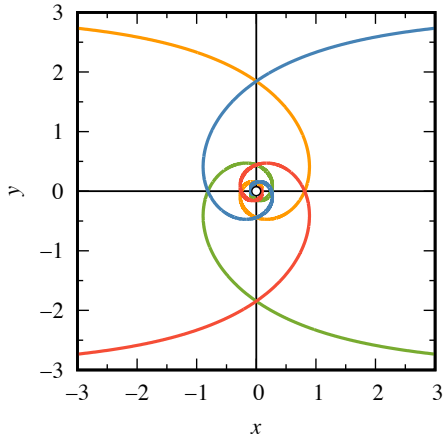


FIG. 5. Timelike geodesics (Poincaré spirals) with the radial time t given in units of t_0 and $\kappa = 1/3$, corresponding to the curves in the previous figure. The blue and green (orange and red) lines are moving away (towards) from (to) the singularity. Furthermore, particles following the trajectories in the first (third) and second (fourth) quadrants are spinning clockwise (counterclockwise). The blank point at the origin is just to emphasize that the curves do not reach the singularity.

is perpendicular to both the director $\hat{\mathbf{n}}$ (i.e. the unit vector along the average orientation of the molecular rods constituting the nematic medium) and the wave vector \mathbf{k} . In this case, light propagates as in an isotropic medium of refractive index n_o with velocity c/n_o . As for the extraordinary ray, the polarization lies in the plane formed by $\hat{\mathbf{n}}$ and \mathbf{k} . Further, the direction of the Poynting vector \mathbf{S} differs from the direction of \mathbf{k} , which means that the energy velocity differs from the phase velocity, leading to

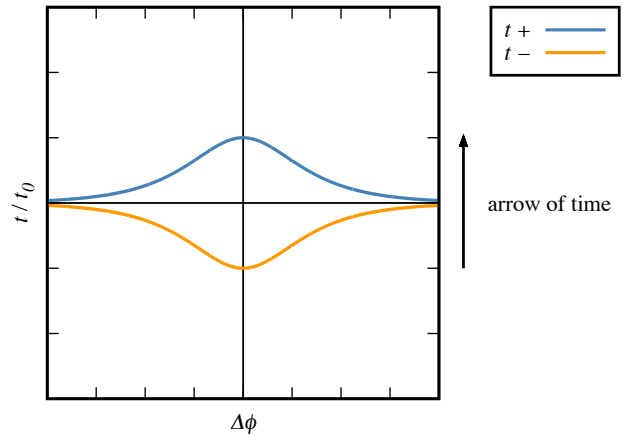


FIG. 6. Graph for the geodesic equation given by Eq. (51) with t in units of t_0 , with the blue curve for the upper cone and the orange curve for the lower one. A tachyon coming from the singularity (from the left of the graph) with $J > 0$ accelerates until the end of its time $t = t_0$ and then decelerates towards to the singularity being ultimately annihilated. This creates a tachyon on the other sheet which goes through the same process.

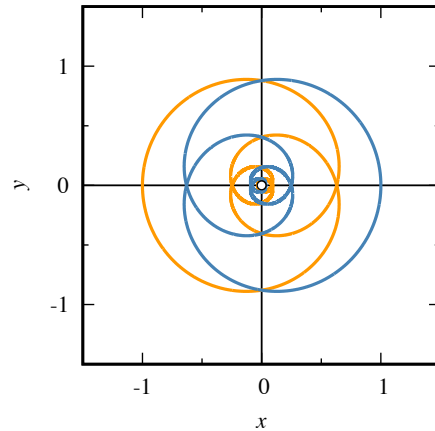


FIG. 7. Spacelike geodesics (Poincaré spirals) with radial time t given in units of t_0 and $\kappa = 1/3$, corresponding to the curves in the previous figure. The closed curves shows that tachyons spiral outward from the singularity and inward to the singularity on the same sheet of the cone.

two different refractive indexes: the ray index N_r , associated to the energy velocity, and the phase index N_p , associated with the phase velocity [24]. In this work, we discuss only the extraordinary ray.

The application of Fermat's principle to the extraordinary light grants us the path followed by the energy. Therefore, the effective refractive index N_e in Eq. (54) is the ray index N_r and is given by [25]

$$N_r^2 = n_o^2 \cos^2 \beta + n_e^2 \sin^2 \beta, \quad (55)$$

where β is the angle between the director $\hat{\mathbf{n}}$ and the

Poynting vector \mathbf{S} .

Fermat's principle essentially sums up to the geodesic determination by requiring $\delta \int_A^B \gamma_{ij} dx^i dx^j = 0$. Therefore, we may think of the curved trajectories of light rays in an anisotropic material as geodesics which can be found from the identification

$$N_r^2 dl^2 = \gamma_{ij} dx^i dx^j, \quad (56)$$

where we introduce the γ_{ij} notation to emphasize that we are dealing with a three dimensional metric. The angle β is determined from the specific configurations of the director field $\hat{\mathbf{n}}$ as follows. If the curve $\mathbf{r}(\lambda)$, where λ is a parameter along the curve, represents the light trajectory, then

$$\mathbf{t}(\lambda) = \frac{d\mathbf{r}}{d\lambda} \quad (57)$$

is the tangent vector at each position parameterized by λ . If the parameter λ is the arc length l , then from the theory of the differential geometry of curves [26], $\|\mathbf{t}\| = 1$. Thus, fixing this choice $\lambda = l$ and also using the fact that $\|\hat{\mathbf{n}}\| = 1$,

$$\cos \beta = \mathbf{t} \cdot \hat{\mathbf{n}}. \quad (58)$$

To proceed further, one has to know the expression for the director $\hat{\mathbf{n}}$, which depends on the system in question. In what follows, we show the form for $\hat{\mathbf{n}}$ that is suitable for our cosmological analog model. The hyperbolic behavior of the metamaterial is characterized by a topological defect called disclination. In our case, the liquid crystal is in a nematic phase and such disclinations are classified according to the topological index (or strength) k which gives a measure of how much the director $\hat{\mathbf{n}}$ rotates as one goes around the defect. Thus, following the same approach as Refs. [27–29], the director configurations (in the xy plane) are given by

$$\vartheta(\phi) = k\phi + c, \quad (59)$$

where ϑ is the angle between the molecular axis and the x -axis, ϕ is the usual azimuthal angle in cylindrical or spherical coordinates and c is a constant parameter. In the case discussed here, the disclinations are such that the system presents a translational symmetry along the z -axis. Therefore, we have effectively a two dimensional problem and the director $\hat{\mathbf{n}}$ is given in Cartesian coordinates by [27–29]

$$\hat{\mathbf{n}} = (\cos \vartheta, \sin \vartheta, 0). \quad (60)$$

In order to simulate Klein-Gordon (KG) particles in a Milne universe, let us consider a radial director field (see FIG. 8)

$$\hat{\mathbf{n}} = (\cos \phi, \sin \phi, 0), \quad (61)$$

where in this case $k = 1$ and $c = 0$ in Eq. (59). For convenience we will use cylindrical coordinates (ρ, ϕ, z) ,

where $\mathbf{r}(l) = \rho \hat{\boldsymbol{\rho}} + z \hat{\mathbf{z}}$ and $\hat{\mathbf{n}} = \hat{\boldsymbol{\rho}}$ by Eq. (61). Therefore, the tangent vector \mathbf{t} will be

$$\mathbf{t} = \frac{d\mathbf{r}}{dl} = \dot{\rho} \hat{\boldsymbol{\rho}} + \rho \dot{\phi} \hat{\boldsymbol{\phi}} + \dot{z} \hat{\mathbf{z}}, \quad (62)$$

where the dot stands for d/dl . Then, from Eq. (58) we have

$$\cos \beta = \dot{\rho}. \quad (63)$$

Next, let us consider the Euclidean line element

$$dl^2 = d\rho^2 + \rho^2 d\phi^2 + dz^2, \quad (64)$$

which leads to the following relation

$$\dot{\rho}^2 + \rho^2 \dot{\phi}^2 + \dot{z}^2 = 1. \quad (65)$$

Therefore, combining Eqs. (63) and (65) one gets

$$\sin \beta = \sqrt{\rho^2 \dot{\phi}^2 + \dot{z}^2}. \quad (66)$$

The ray index N_r can now be obtained with the help of Eqs. (55), (63) and (66) as

$$N_r^2 = n_o^2 \dot{\rho}^2 + n_e^2 (\rho^2 \dot{\phi}^2 + \dot{z}^2). \quad (67)$$

Then, the line element $ds^2 = N_r^2 dl^2 = \gamma_{ij} dx^i dx^j$ will have the following form

$$ds^2 = n_o^2 d\rho^2 + n_e^2 \rho^2 d\phi^2 + n_e^2 dz^2. \quad (68)$$

Because we are dealing with metamaterials, it is more useful to write the refractive indexes n_o and n_e as functions of the components of the permittivity tensor ϵ_{ij} of the material. Therefore, introducing the usual notation, as in Ref. [30], where $n_o^2 = \epsilon_{\perp}$ and $n_e^2 = \epsilon_{\parallel}$, Eq. (68) becomes

$$ds^2 = \epsilon_{\perp} d\rho^2 + \epsilon_{\parallel} \rho^2 d\phi^2 + \epsilon_{\parallel} dz^2, \quad (69)$$

where in this case $\epsilon_{\perp} = \epsilon_{\phi\phi} = \epsilon_{zz}$ and $\epsilon_{\parallel} = \epsilon_{\rho\rho}$. Furthermore, the permittivity tensor ϵ is given by [24, 25]

$$\epsilon = \epsilon_{\parallel} \hat{\boldsymbol{\rho}} \otimes \hat{\boldsymbol{\rho}} + \epsilon_{\perp} \hat{\boldsymbol{\phi}} \otimes \hat{\boldsymbol{\phi}} + \epsilon_{\perp} \hat{\mathbf{z}} \otimes \hat{\mathbf{z}}. \quad (70)$$

As pointed out before, the system in question has a translational symmetry along the z -axis, and therefore we are interested in the extraordinary ray propagating in $z = \text{constant}$ planes. Thus, $dz = 0$ in Eq. (69). Furthermore, the metric tensor γ_{ij} describes a “real” three-dimensional space, having only spatial coordinates. However, light propagates along null geodesics in a four-dimensional spacetime. Therefore, we use the fact that the application of Fermat's principle in a three-dimensional metric with only spatial coordinates is equivalent to calculating null geodesics in a four-dimensional spacetime with a pseudo-Riemannian metric g_{ij} . Thus, the relation between the metrics γ_{ij} and g_{ij} is as follows (see p. 1108 of Ref. [12])

$$\gamma_{ij} = -\frac{g_{ij}}{g_{00}}. \quad (71)$$

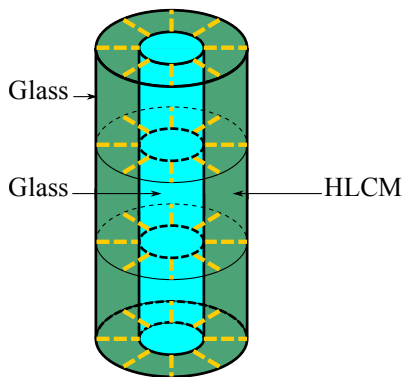


FIG. 8. Director configurations for HLCM in a cylindrical shell, with optical axis represented in cylindrical coordinates (ρ, ϕ, z) as $\hat{\mathbf{n}} = \hat{\rho}$. The walls of the inner and outer cylinders are made of glass, while the liquid crystal together with metallic nanorods (aligned in the direction of $\hat{\mathbf{n}}$) fills the space in between.

Taking $g_{00} = 1$, Eq. (69) becomes

$$ds^2 = dT^2 - \epsilon_{\perp} d\rho^2 - \epsilon_{\parallel} \rho^2 d\phi^2, \quad (72)$$

where T is the Minkowskian time.

In what follows, we explore the property of metamaterials to produce negative permittivities. Due to the fact the director field is radial ($\hat{\mathbf{n}} = \hat{\rho}$) and the metallic nanorods are aligned in the same direction, we have a metallic behavior along the radial coordinate and can therefore obtain $\epsilon_{\parallel} < 0$. Furthermore, considering $\epsilon_{\perp} > 0$ and rescaling the radial coordinate by $r = \rho\sqrt{\epsilon_{\perp}}$ one gets

$$ds^2 = dT^2 - dr^2 + \alpha^2 r^2 d\phi^2, \quad (73)$$

where $\alpha^2 = |\epsilon_{\parallel}|/\epsilon_{\perp}$ is the disclination parameter associated to a hyperbolic (imaginary) deficit angle of $i \times 2\pi\alpha$ [31]. Also note that the spatial part of the metric above is equivalent to the \mathcal{M}_C metric given by Eq. (23), with r behaving as the timelike variable T .

By the same procedure developed in the previous section, Eq. (73) gives the Lagrangian

$$\mathcal{L}_{\text{kin}} = \frac{\dot{T}^2}{2} - \frac{\dot{r}^2}{2} + \frac{\alpha^2 r^2 \dot{\phi}^2}{2}, \quad (74)$$

which leads to the following geodesic equations

$$\frac{dT}{d\lambda} = \nu, \quad (75)$$

$$\ddot{\phi} + \frac{2}{r} \dot{r} \dot{\phi} = 0, \quad (76)$$

$$\ddot{r} + \alpha^2 r \dot{\phi}^2 = 0, \quad (77)$$

where λ is an affine parameter and ν is a constant. The first equation just states the conservation of the canonical momentum p_T , while the other two are equivalent to the geodesic equations for classical particles in \mathcal{M}_C given by Eqs. (36) and (37). It is possible to follow the same steps

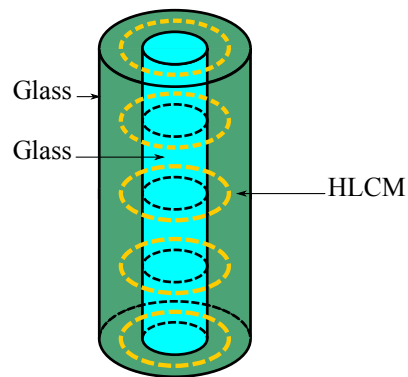


FIG. 9. Director configurations for HLCM in a cylindrical shell for a circular field, with optical axis represented in cylindrical coordinates (ρ, ϕ, z) as $\hat{\mathbf{n}} = \hat{\phi}$.

to integrate the equations as we did in Sec. III. However, as in this case we are dealing with null geodesics, $g_{ij}\dot{x}^i\dot{x}^j = 0$ and therefore one gets the following useful constraint

$$\dot{r}^2 - \frac{\alpha^2 L^2}{r^2} = \nu^2, \quad (78)$$

with the constant $L = r^2 \dot{\phi}$ being the angular momentum. The previous equation is essentially the same as Eq. (39). The geodesic equations for this case were already solved in Ref. [31] and the solution for the trajectory is the following

$$r = \frac{\alpha r_0}{|\sinh \alpha \Delta\phi|}, \quad (79)$$

where $r_0 = |L|/\nu$. As a result, the path followed by light rays in the three-dimensional space in the metamaterial are Poincaré's spirals like the timelike geodesics in \mathcal{M}_C found in Sec. III. Comparing Eqs. (46) and (79), the radial coordinate r behaves like the time coordinate t and α is the analogue of the constant κ . As pointed out in Ref. [31], the hyperbolic behavior of the material generates a force towards the defect and the parameter α is directly related to it, with $1/\alpha$ being understood as the vorticity of the defect (the smaller the value of α , the stronger is the attraction towards the defect). Furthermore, since the defect generates an attraction, the trajectories given by Eq. (79) can be interpreted as the equivalent to geodesics in \mathcal{M}_C going to the cosmic singularity (big crunch).

To simulate tachyons, we consider the director field as $\hat{\mathbf{n}} = \hat{\phi}$ (see FIG. 9), meaning that $k = 1$ and $c = \pi/2$ in Eq. (60). In this case, our four-dimensional line element will be

$$ds^2 = dT^2 - \epsilon_{\parallel} d\rho^2 - \epsilon_{\perp} \rho^2 d\phi^2, \quad (80)$$

where now $\epsilon_{\parallel} = \epsilon_{\phi\phi}$ and $\epsilon_{\perp} = \epsilon_{\rho\rho}$. Thus, considering $\epsilon_{\parallel} < 0$, $\epsilon_{\perp} > 0$ and rescaling the radial coordinate by $r = \rho\sqrt{|\epsilon_{\parallel}|}$ one gets

$$ds^2 = dT^2 + dr^2 - \alpha^2 r^2 d\phi^2, \quad (81)$$

where $\alpha^2 = \epsilon_{\perp}/|\epsilon_{\parallel}|$. Therefore, the Lagrangian will be

$$\mathcal{L}_{\text{kin}} = \frac{\dot{T}^2}{2} + \frac{\dot{r}^2}{2} - \frac{\alpha^2 r^2 \dot{\phi}^2}{2}, \quad (82)$$

which also gives Eqs. (75), (76), (77) as geodesic equations. However, as in Sec. III we will have a different constraint. Thus, for $g_{ij}\dot{x}^i\dot{x}^j = 0$,

$$\dot{r}^2 - \frac{\alpha^2 L^2}{r^2} = -\nu^2, \quad (83)$$

which is the analogue of Eq. (48). By the same procedure done in the previous cases, the trajectory will be

$$r = \frac{\alpha r_0}{\cosh \alpha \Delta \phi}, \quad (84)$$

where $r_0 = |L|/\nu$ again. Therefore, we obtain the analogue of the spacelike geodesics in \mathcal{M}_C found in Sec. III.

Having shown that the classical behavior can be emulated, in the following section it will be shown that the quantum behavior of KG particles in \mathcal{M}_C also has an analogy in the framework of wave optics.

V. MIMICKING QUANTUM PARTICLES IN \mathcal{M}_C

In this last section, our goal is to show how to mimic a KG particle in \mathcal{M}_C through the system presented in the previous section. Therefore, let us consider the KG equation for a scalar field φ (in natural units $c, \hbar = 1$)

$$(\Delta - m^2) \varphi = 0, \quad (85)$$

where Δ is the Laplace-Beltrami operator as presented in Sec. II. For the \mathcal{M}_C universe, $\Delta_{\mathcal{M}_C}$ was given in Eq. (27). Thus,

$$\left[-\frac{1}{t} \frac{\partial}{\partial t} \left(t \frac{\partial}{\partial t} \right) + \frac{1}{\kappa^2 t^2} \frac{\partial^2}{\partial \phi^2} - m^2 \right] \varphi = 0. \quad (86)$$

Concerning the metamaterial model, we examine the propagation of light in the scalar wave approximation, allowing the use of the covariant d'Alembert wave equation

$$\nabla_i \nabla^i \Phi = \frac{1}{\sqrt{-g}} \partial_i (\sqrt{-g} g^{ij} \partial_j \Phi) = 0, \quad (87)$$

where Φ is the wave function. Therefore, according to the metric given by Eq. (72), one gets

$$-\frac{1}{\epsilon_{\perp}} \frac{1}{\rho} \frac{\partial}{\partial \rho} \left(\rho \frac{\partial \Phi}{\partial \rho} \right) - \frac{1}{\epsilon_{\parallel}} \frac{1}{\rho^2} \frac{\partial^2 \Phi}{\partial \phi^2} + \frac{\partial^2 \Phi}{\partial T^2} = 0. \quad (88)$$

Assuming a harmonic dependence in time, we make a separation of variables $\Phi(t, \rho, \phi) = e^{-i\omega T} \psi(\rho, \phi)$. Thus,

$$-\frac{1}{\epsilon_{\perp}} \frac{1}{\rho} \frac{\partial}{\partial \rho} \left(\rho \frac{\partial \psi}{\partial \rho} \right) - \frac{1}{\epsilon_{\parallel}} \frac{1}{\rho^2} \frac{\partial^2 \psi}{\partial \phi^2} - \omega^2 \psi = 0, \quad (89)$$

where ω is the propagation frequency of the light or effective mass of an analogue KG particle. Furthermore, recalling our previous choice of $\epsilon_{\perp} = \epsilon_{\phi\phi} > 0$ and $\epsilon_{\parallel} = \epsilon_{\rho\rho} < 0$, one gets

$$\left[-\frac{1}{\epsilon_{\perp}} \frac{1}{\rho} \frac{\partial}{\partial \rho} \left(\rho \frac{\partial}{\partial \rho} \right) + \frac{1}{|\epsilon_{\parallel}|} \frac{1}{\rho^2} \frac{\partial^2}{\partial \phi^2} - \omega^2 \right] \psi = 0. \quad (90)$$

The equation above is similar to Eq. (86) and it was already used to mimic KG particles in plasmonic metamaterials [7, 9]. In terms of $r = \rho\sqrt{\epsilon_{\perp}}$ and the parameter $\alpha^2 = |\epsilon_{\parallel}|/\epsilon_{\perp}$, it becomes

$$\left[-\frac{1}{r} \frac{\partial}{\partial r} \left(r \frac{\partial}{\partial r} \right) + \frac{1}{\alpha^2} \frac{1}{r^2} \frac{\partial^2}{\partial \phi^2} - \omega^2 \right] \psi = 0, \quad (91)$$

where ω is treated as an effective mass (in natural units). Furthermore, there is a contribution α^2 from the disclination, which by Eq. (26) is associated to a cone angle $\theta = \sin^{-1} \alpha$, whereas in Eq. (86) $\theta = \sinh^{-1} \kappa$.

To solve Eq. (91), we remark that the hyperbolic metamaterial obeys the dispersion relation

$$\frac{k_{\rho}^2}{\epsilon_{\perp}} - \frac{k_{\phi}^2}{|\epsilon_{\parallel}|} = \omega^2 \quad (92)$$

and the angular momentum conservation $l = k_{\phi}\rho$, as shown in Ref. [6]. In terms of the angular momentum quantum number l and the radial variable r , Eq. (92) becomes

$$k_r^2 - \frac{l^2}{\alpha^2 r^2} - \omega^2 = 0, \quad (93)$$

where we have used the fact that $k_r = k_{\rho}/\sqrt{\epsilon_{\perp}}$ due to the change of scale passing from ρ to r . Eq. (93) is consistent with Eq. (91) since, in terms of operators, it takes the following form

$$\left[\hat{k}_r^2 - \frac{\hat{L}_z^2}{\alpha^2 r^2} - \omega^2 \right] \psi = 0, \quad (94)$$

where \hat{k}_r^2 and \hat{L}_z^2 are the usual operators

$$\hat{k}_r^2 = -\frac{1}{r} \frac{\partial}{\partial r} \left(r \frac{\partial}{\partial r} \right), \quad (95)$$

$$\hat{L}_z^2 = -\frac{\partial^2}{\partial \phi^2}. \quad (96)$$

Therefore, separating the variables $\psi(r, \phi) = f(r)g(\phi)$ leads to the equations

$$\frac{d^2 g}{d\phi^2} + l^2 g = 0, \quad (97)$$

and

$$r^2 \frac{d^2 f}{dr^2} + r \frac{df}{dr} + \left(\omega^2 r^2 + \frac{l^2}{\alpha^2} \right) f = 0. \quad (98)$$

Thus, the solution for Eq. (97) is

$$g(\phi) = Ae^{i\phi} + Be^{-i\phi}, \quad (99)$$

where A, B are constants of integration. As for Eq. (98), it is a Bessel differential equation of imaginary order il/α with solutions [32, 33]

$$f(r) = C\tilde{J}_{l/\alpha}(\omega r) + D\tilde{Y}_{l/\alpha}(\omega r), \quad (100)$$

which C, D being constants of integration and $\tilde{J}_{l/\alpha}, \tilde{Y}_{l/\alpha}$ are linearly independent solutions defined in Ref. [32] as

$$\tilde{J}_{l/\alpha} = \operatorname{sech}\left(\frac{\pi l}{2\alpha}\right) \operatorname{Re} J_{il/\alpha}(\omega r), \quad (101)$$

$$\tilde{Y}_{l/\alpha} = \operatorname{sech}\left(\frac{\pi l}{2\alpha}\right) \operatorname{Re} Y_{il/\alpha}(\omega r), \quad (102)$$

where $\operatorname{Re} J_{il/\alpha}$ and $\operatorname{Re} Y_{il/\alpha}$ are the real parts of Bessel and Neumann functions, respectively. Following the same procedure for Eq. (86), one gets the same solutions for the scalar field φ (as obtained in Ref. [17]) with the variable r replaced by t and the constants ω, α interchanged by m, κ , respectively.

An interesting feature [32, 33] of the Eqs. (101), (102) is that they oscillate rapidly near the origin, as one can see from its behavior as $r \rightarrow 0^+$

$$\begin{aligned} \tilde{J}_{l/\alpha}(\omega r) &= \left(\frac{\tanh(\pi l/2\alpha)}{\pi l/2\alpha}\right)^{1/2} \cos\left[\frac{l}{\alpha} \ln\left(\frac{\omega r}{2}\right) - \gamma_{l/\alpha}\right] \\ &\quad + O(\omega^2 r^2), \end{aligned} \quad (103)$$

$$\begin{aligned} \tilde{Y}_{l/\alpha}(\omega r) &= \left(\frac{\coth(\pi l/2\alpha)}{\pi l/2\alpha}\right)^{1/2} \sin\left[\frac{l}{\alpha} \ln\left(\frac{\omega r}{2}\right) - \gamma_{l/\alpha}\right] \\ &\quad + O(\omega^2 r^2), \end{aligned} \quad (104)$$

where $\gamma_{l/\alpha}$ is a constant defined as $\gamma_{l/\alpha} \equiv \arg \Gamma(1+il/\alpha)$, with Γ being the Gamma function. The rapid oscillations are due to the logarithmic argument of the trigonometric functions. Also, for a fixed l , the smaller the value of α , the stronger the oscillations become (reducing the value of α ‘‘squeezes’’ the period of the trigonometric functions). This is the analogous of the classical behavior in Sec. IV where $1/\alpha$ is related to the vorticity.

Furthermore, for $l \neq 0$ Eqs. (101), (102) are not continuous through the origin, which is similar to the classical geodesics that in general do not cross the singularity. In Ref. [17] it was given an interesting interpretation for this fact constructing a Hilbert space $\mathcal{H} = \mathcal{H}^{(-)} \oplus \mathcal{H}^{(+)}$ as a direct sum of two Hilbert spaces $\mathcal{H}^{(-)}, \mathcal{H}^{(+)}$. The elements of $\mathcal{H}^{(-)}$ are solutions of Eq. (86) in the pre-singularity era ($t < 0$) while the ones of $\mathcal{H}^{(+)}$ are solutions in the post-singularity era ($t > 0$). That is, $\mathcal{H} = \mathcal{H}^- \oplus \mathcal{H}^+$ is a vector space whose elements φ have the following form [34]

$$\varphi = \left(\varphi^{(-)}, \varphi^{(+)}\right) \in \mathcal{H}^{(-)} \times \mathcal{H}^{(+)}, \quad (105)$$

with an inner product

$$\langle \varphi | \psi \rangle = \left\langle \varphi^{(-)} | \psi^{(-)} \right\rangle + \left\langle \varphi^{(+)} | \psi^{(+)} \right\rangle. \quad (106)$$

Hence, vectors like $(\varphi^{(-)}, 0)$ and $(0, \varphi^{(+)})$ describe states of annihilation and creation of particles at the singularity $t = 0$, respectively. By Eq. (106) an inner product between those kinds of states yields zero, which means no correlation between them. This reflects the loss of phase of the wave function due to the strong oscillations around the singularity.

The $l = 0$ case is rather straightforward; from Eqs. (99), (101) and (102), $g(\phi)$ is constant and the Bessel functions of imaginary order reduce to the usual ones $J_0(\omega r), Y_0(\omega r)$. Moreover, due to the fact that in the classical case the geodesics are straight lines crossing the singularity and knowing that Y_0 diverges at the origin, a more satisfactory physical solution is given by J_0 , as it is continuous and well-defined at the origin (singularity) $r = 0$ ($t = 0$).

Next, we consider briefly the case of tachyons. Therefore, as pointed in Ref. [22] tachyons can be regarded as having an imaginary ‘‘rest’’ mass $m = i\mu$, with $\mu \in \mathbb{R}$. As a result, Eq. (86) becomes

$$\left[-\frac{1}{t} \frac{\partial}{\partial t} \left(t \frac{\partial}{\partial t}\right) + \frac{1}{\kappa^2 t^2} \frac{\partial^2}{\partial \phi^2} + \mu^2\right] \varphi = 0. \quad (107)$$

To mimic tachyons in the metamaterial we consider again the case of a circular director field $\hat{\mathbf{n}} = \hat{\phi}$ as in the previous section. Therefore, substituting the metric (81) in the covariant d’Alembert wave equation (87) and considering $\Phi(t, r, \phi) = e^{-i\omega T} \psi(r, \phi)$, one gets

$$\left[-\frac{1}{r} \frac{\partial}{\partial r} \left(r \frac{\partial}{\partial r}\right) + \frac{1}{\alpha^2 r^2} \frac{\partial^2}{\partial \phi^2} + \omega^2\right] \psi = 0, \quad (108)$$

or, in the operator form

$$\left[\hat{k}_r^2 - \frac{\hat{L}_z^2}{\alpha^2 r^2} + \omega^2\right] \psi = 0, \quad (109)$$

where $\alpha^2 = \epsilon_{\perp}/|\epsilon_{\parallel}| = \epsilon_{\rho\rho}/|\epsilon_{\phi\phi}|$ and ω is the analogue of $\operatorname{Im} m = \mu$. The dispersion relation in this case takes the form

$$-\frac{k_{\rho}^2}{|\epsilon_{\parallel}|} + \frac{k_{\phi}^2}{\epsilon_{\perp}} = \omega^2. \quad (110)$$

Hence, in terms of the angular momentum l , the constant α and $k_r = k_{\rho}/\sqrt{|\epsilon_{\parallel}|}$, Eq. (110) becomes

$$k_r^2 - \frac{l^2}{\alpha^2 r^2} + \omega^2 = 0, \quad (111)$$

which is consistent with Eq. (109).

Thus, separating the variables as $\psi(r, \phi) = f(r)g(\phi)$ one gets the same solution given by Eq. (99) for $g(\phi)$. As for the radial part,

$$r^2 \frac{d^2 f}{dr^2} + r \frac{df}{dr} - \left(\omega^2 r^2 - \frac{l^2}{\alpha^2}\right) f = 0. \quad (112)$$

which is the modified Bessel differential equation with imaginary order il/α . The solution for this case will be

$$f(r) = C\tilde{I}_{l/\alpha}(\omega r) + D\tilde{K}_{l/\alpha}(\omega r), \quad (113)$$

where we kept the notation of Ref. [32], with $\tilde{I}_{l/\alpha} = \text{Re } I_{il/\alpha}$ and $\tilde{K}_{l/\alpha} = \tilde{K}_{il/\alpha}$. The functions $I_{il/\alpha}$, $K_{il/\alpha}$ are the modified Bessel functions of first and second kind, respectively. As in the previous case, their behavior near the origin is characterized by rapid oscillations. However, their asymptotic behavior is exponential [32, 33],

$$\tilde{I}_{l/\alpha}(\omega r) = \left(\frac{1}{2\pi\omega r}\right)^{1/2} e^{\omega r} \left[1 + O\left(\frac{1}{\omega r}\right)\right], \quad (114)$$

$$\tilde{K}_{l/\alpha}(\omega r) = \left(\frac{\pi}{2\omega r}\right)^{1/2} e^{-\omega r} \left[1 + O\left(\frac{1}{\omega r}\right)\right]. \quad (115)$$

Therefore, since the classical trajectories shown in FIGs. 6, 7 indicate the idea of bound states, a more appropriate physical solution is $\tilde{K}_{l/\alpha}$.

As a last remark, we advise that there was an unfortunate error in Ref. [31], where an equation similar to Eq. (91) was solved. The solution for that case also will be in the form of $\psi(r, \phi) = f(r)g(\phi)$, with $f(r)$ and $g(\phi)$ given by Eqs. (100) and (99), respectively.

VI. CONCLUSIONS

The possibility of doing experiments in condensed matter systems that simulate cosmological scenarios was pro-

posed here with the particular focus on the Milne compactified universe \mathcal{M}_C . We have shown that both Klein-Gordon particles and tachyons in \mathcal{M}_C can be nicely represented by ordinary light propagating in specially engineered materials known as hyperbolic metamaterials. Within the realm of geometrical optics, we pointed out that the classical trajectories of those particles can be perfectly matched to light ray paths in the metamaterial, while the quantum wave functions may be realized by wave optics. We remark the exciting possibility of experimentally checking, not only the trajectories, but also the lack of correlation between the wave function of particles on both sides of the cosmological transition, through the analogue model presented here. Finally, further theoretical results can be found through the study of wave scattering, applying the method of partial waves [29] to the present model. This is presently under investigation and will be the theme of a separate publication.

ACKNOWLEDGMENTS

D.F. and F.M. are thankful for the financial support and warm hospitality of the group at Université de Lorraine where this work was conceived and partly done. This work has been partially supported by CNPq, CAPES and FACEPE (Brazilian agencies).

-
- [1] P. J. Steinhardt and N. Turok, ‘‘Cosmic evolution in a cyclic universe,’’ *Physical Review D*, vol. 65, no. 12, p. 126003, 2002.
 - [2] G. T. Horowitz and A. R. Steif, ‘‘Singular string solutions with nonsingular initial data,’’ *Physics Letters B*, vol. 258, no. 1, pp. 91–96, 1991.
 - [3] V. Veselago, ‘‘The electrodynamics of substances with simultaneously negative values of ϵ and μ ,’’ *Soviet physics uspekhi*, vol. 4, no. 10, p. 509, 1968.
 - [4] J. Pendry, S. D. and S. DR, ‘‘Controlling electromagnetic fields,’’ *Science*, vol. 312, no. 5781, pp. 1780–1782, 2006.
 - [5] A. Poddubny, I. Iorsh, P. Belov, and Y. Kivshar, ‘‘Hyperbolic metamaterials,’’ *Nature photonics*, vol. 7, pp. 958–967, 2013.
 - [6] Z. Jacob, L. V. Alekseyev, and E. Narimanov, ‘‘Optical hyperlens: far-field imaging beyond the diffraction limit,’’ *Optics express*, vol. 14, no. 18, pp. 8247–8256, 2006.
 - [7] I. I. Smolyaninov, Y. J. Hung, and E. Hwang, ‘‘Experimental modeling of cosmological inflation with metamaterials,’’ *Physics Letters A*, vol. 376, no. 38, pp. 2575–2579, 2012.
 - [8] I. I. Smolyaninov and E. E. Narimanov, ‘‘Metric signature transitions in optical metamaterials,’’ *Phys. Rev. Lett.*, vol. 105, p. 067402, 2010.
 - [9] I. I. Smolyaninov and Y. J. Hung, ‘‘Modeling of time with metamaterials,’’ *JOSA B*, vol. 28, no. 7, pp. 1591–1595, 2011.
 - [10] D. Figueiredo, F. A. Gomes, S. Fumeron, B. Berche, and F. Moraes, ‘‘Modeling kleinian cosmology with electronic metamaterials,’’ *Physical Review D*, vol. 94, no. 4, p. 044039, 2016.
 - [11] M. P. d. Carmo, *Differential geometry of curves and surfaces*. Prentice-Hall, 1976.
 - [12] C. W. Misner, K. S. Thorne, and J. A. Wheeler, *Gravitation*. Macmillan, 1973.
 - [13] Ø. Grøn and S. Hervik, *Einstein’s general theory of relativity: with modern applications in cosmology*. Springer Science & Business Media, 2007.
 - [14] J. Khoury, B. A. Ovrut, N. Seiberg, P. J. Steinhardt, and N. Turok, ‘‘From big crunch to big bang,’’ *Physical Review D*, vol. 65, no. 8, p. 086007, 2002.
 - [15] A. J. Tolley, N. Turok, and P. J. Steinhardt, ‘‘Cosmological perturbations in a big-crunch–big-bang space-time,’’ *Physical Review D*, vol. 69, no. 10, p. 106005, 2004.
 - [16] P. Małkiewicz and W. Piechocki, ‘‘A simple model of big-crunch/big-bang transition,’’ *Classical and Quantum Gravity*, vol. 23, no. 9, p. 2963, 2006.
 - [17] P. Małkiewicz and W. Piechocki, ‘‘Probing the cosmological singularity with a particle,’’ *Classical and Quantum*

- Gravity*, vol. 23, no. 23, p. 7045, 2006.
- [18] L. Baulieu, J. de Boer, B. Pioline, and E. Rabinovici, *Proceedings of the NATO Advanced Institute on String Theory: From Gauge Interactions to Cosmology*, vol. 208. Springer Science & Business Media, 2006.
- [19] L. Landau and E. Lifshitz, *The classical theory of fields*. Elsevier, 2013.
- [20] J. D. Lawrence, *A catalog of special plane curves*. Dover Publications, 2014.
- [21] K. Kowalski and J. Rembieliński, “On the dynamics of a particle on a cone,” *Annals of Physics*, vol. 329, pp. 146–157, 2013.
- [22] G. Feinberg, “Possibility of faster-than-light particles,” *Phys. Rev.*, vol. 159, pp. 1089–1105, Jul 1967.
- [23] J. Xiang and O. D. Lavrentovich, “Liquid crystal structures for transformation optics,” *Molecular Crystals and Liquid Crystals*, vol. 559, no. 1, pp. 106–114, 2012.
- [24] G. R. Fowles, *Introduction to modern optics*. Dover Publications, 1989.
- [25] M. Born and E. Wolf, *Principles of optics: electromagnetic theory of propagation, interference and diffraction of light*. Cambridge University Press, 7th ed., 1999.
- [26] T. J. Willmore, *An introduction to differential geometry*. Dover Publications, 2012.
- [27] C. Sátiro and F. Moraes, “Lensing effects in a nematic liquid crystal with topological defects,” *The European Physical Journal E*, vol. 20, no. 2, pp. 173–178, 2006.
- [28] C. Sátiro and F. Moraes, “On the deflection of light by topological defects in nematic liquid crystals,” *The European Physical Journal E*, vol. 25, no. 4, pp. 425–429, 2008.
- [29] E. Pereira and F. Moraes, “Diffraction of light by topological defects in liquid crystals,” *Liquid Crystals*, vol. 38, no. 3, pp. 295–302, 2011.
- [30] M. Kleman and O. D. Lavrentovich, *Soft matter physics: an introduction*. Springer Science & Business Media, 2007.
- [31] S. Fumeron, B. Berche, F. Santos, E. Pereira, and F. Moraes, “Optics near a hyperbolic defect,” *Physical Review A*, vol. 92, no. 6, p. 063806, 2015.
- [32] F. W. Olver, D. W. Lozier, R. F. Boisvert, and C. W. Clark, *NIST handbook of mathematical functions*. Cambridge University Press, 2010.
- [33] T. Dunster, “Bessel functions of purely imaginary order, with an application to second-order linear differential equations having a large parameter,” *SIAM Journal on Mathematical Analysis*, vol. 21, no. 4, pp. 995–1018, 1990.
- [34] E. Prugovecki, *Quantum mechanics in Hilbert space*, vol. 92. Academic Press, 1982.